Theoretical Study of the Initial Decomposition Process of the Energetic Material Urea Nitrate

Yuji Kohno,[†,‡] Osamu Takahashi,[†] Reiko I. Hiyoshi,[§] Jun Nakamura,[§] and Ko Saito*[,†]

Department of Chemistry, Graduate School of Science, Hiroshima University, Kagamiyama 1-3-1, Higashi-Hiroshima 739-8526, Japan, and National Research Institute of Police Science, Kashiwanoha 6-3-1, Kashiwa, Chiba 277-0882, Japan

Received: July 18, 2002; In Final Form: June 16, 2003

The initial decomposition process of urea nitrate (UN) was studied by using ab initio calculations. To determine the most favorable reaction pathway of decomposition, geometries, structures, and energies were evaluated for reactants, products, intermediates, and transition states of the proposed pathways at the HF/6-31++G(2d,p), MP2/6-31++G(2d,p), and the B3LYP/6-31++G(2d,p) levels. It has been found that there is a reaction path for the endothermic channel with a potential energy barrier of 47.8 kcal/mol at the MP2/6-31++G(2d,p) level. Although a considerable difference was found between the actual crystal structure and the optimized structure of UN, these results strongly suggest that the decomposition occurs via internal hydrogen transfer from one amino group to the other $-NH_2$ to produce NH_3. This study has revealed a series of the UN reaction paths through one intermediate and two transition states with the evolutions of the initial gaseous species, NH_3, HNCO, and HNO_3, in that order. These calculated results seem to support the experimental results observed at the thermal decomposition of UN by using *T*-jump/FT-IR spectroscopy.

1. Introduction

The molecular design of new energetic materials (e.g., explosives and propellants) with lower sensitivity and higher performance requires an understanding of the mechanisms of the explosion reactions.[1] These mechanisms are still unclear. Urea nitrate (UN, $(NH_2)_2COH^+NO_3^-$) is a considerably stable energetic material that releases a large amount of energy upon explosion. The explosion properties of UN, such as sensitivities and detonation velocity, have been determined recently by Hiyoshi and Nakamura.[2,3] Although many theoretical studies of the urea molecule have been reported previously,[4−11] to our knowledge, there is no publication pertaining to the UN molecule itself. The molecular structure of UN consists of an ion pair (the uronium and nitrate ions), i.e., a cluster. In our previous paper,[12] the density functional theory (DFT) study of the initial decomposition process of the energetic material NTO (5-nitro-2,4-dihydro-3*H*-1,2,4-triazol-3-one) dimer (a cluster) has been reported recently. It has been found that there is a reaction path for the production of CO_2 through the dimer reaction with a potential energy barrier of 87.8 kcal mol^{-1} at the B3LYP/6-31G(d,p) level of theory. This study has revealed a series of NTO dimer reaction paths through four intermediates and five transition states. DFT and the ab initio molecular orbital (MO) method have been shown to be valuable tools to clarify the mechanisms of cluster reactions in energetic materials.

In our previous paper,[13] the thermal decomposition of UN was determined at various conditions by *T*-jump/FT-IR spectroscopy. The behavior of the decomposition products suggests that there are two main decomposition pathways depending on the pressure and temperature. On the basis of these experiments, we postulate that there are two principal reaction channels as follows:

$$[(NH_2)_2COH]NO_3 \rightarrow NH_4NO_3\ (AN)\ (\text{or } NH_3 + HNO_3) + HNCO \quad (1)$$

$$[(NH_2)_2COH]NO_3 \rightarrow N_2O + CO_2 + NH_3 + H_2O \quad (2)$$

The NH_3 from (2) and the HNCO from (1) partially combine to produce NH_4NCO in the gas phase (reaction 3). Isomers of NH_4NCO such as NH_4OCN are also possible:

$$NH_3 + HNCO \rightarrow NH_4NCO \quad (3)$$

The thermochemistry of the two channels was evaluated qualitatively. As a result, it appears that the above two principal reaction channels are possible in the decomposition of UN. These experimental conclusions are supported by the relative concentrations of the species and assignments of the ammonium nitrate (AN) and NH_4NCO species in the spectra of the gas phase. Also, ab initio MO calculations were performed to determine the assignments of unknown frequencies and transition states for the thermal decomposition channels. In the previous study,[13] two transition state structures were determined at the HF/6-31++G(2d,p) level.

The object of the present study was to investigate the relationship between the electronic structure and reactivity of UN. To this end, we performed Hartree−Fock theory (HF), the density functional theory (DFT), and second-order Møller−Plesset perturbation (MP2) calculations to obtain the molecular structure of UN, some related compounds and plausible transition states and to discuss the reactivity of these compounds.

* Corresponding author. Fax: +81-824-24-0727. E-mail: saito@sci.hiroshima-u.ac.jp.
† Hiroshima University.
‡ Present address: Interdisciplinary Shock Wave Research Laboratory, Institute of Fluid Science, Tohoku University, Katahira 2-1-1, Aoba-ku, Sendai, 980-8577, Japan. E-mail: kohno@rainbow.ifs.tohoku.ac.jp.
§ National Research Institute of Police Science.

10.1021/jp026559y CCC: $25.00
Published on Web 07/29/2003

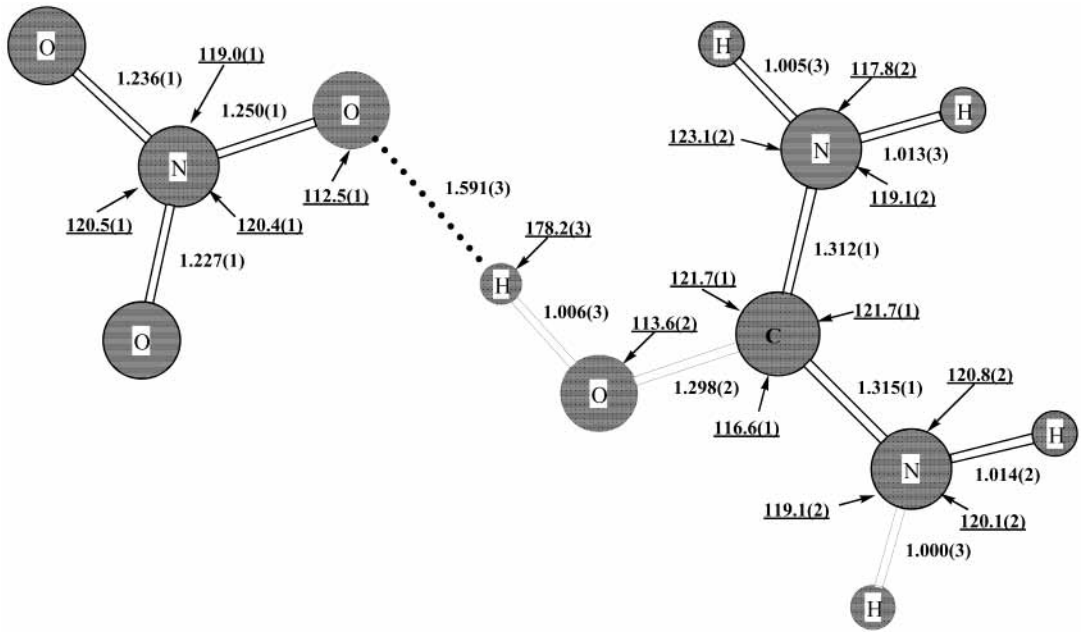

Figure 1. Molecular structure of urea nitrate in the crystalline state.[26] Bond distances are in ångstroms, and angles (underlined) are in degrees. Number in parentheses stand for their standard errors.

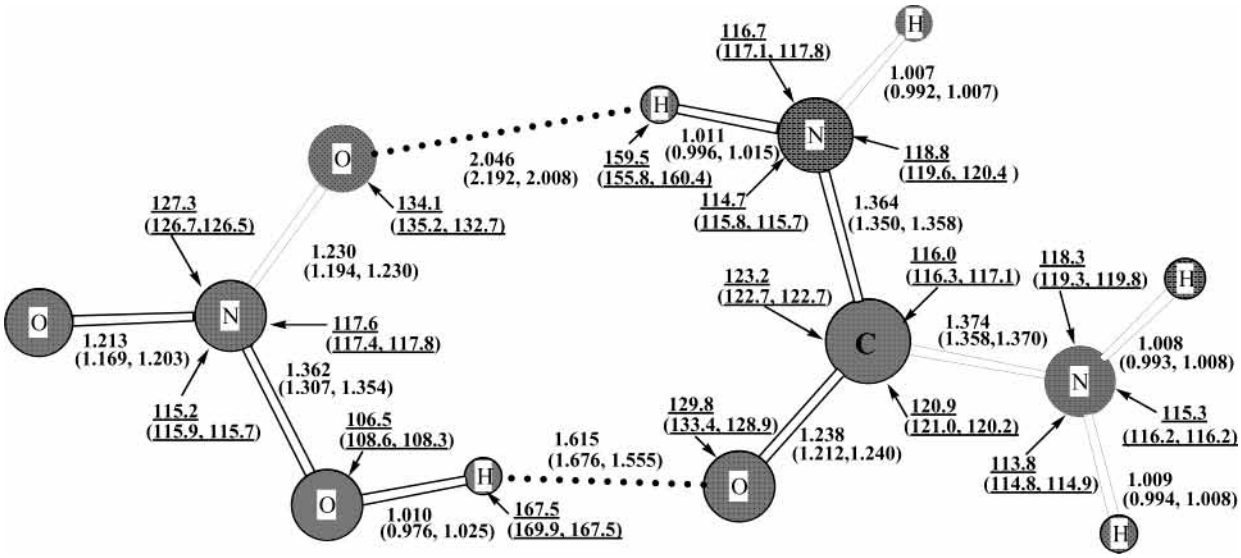

Figure 2. MP2/6-31++G(2d,p) optimized geometry of urea nitrate. Bond distances are in ångstroms, and angles (underlined) are in degrees. Number in parentheses stand for HF/6-31++G(2d,p) optimized values (left-hand side) and B3LYP/6-31++G(2d,p) optimized values (right-hand side).

2. Computational Methods

Ab initio calculations were carried out with the GAUSSIAN-98[14] program package. The basis sets implemented in the program were employed without modification. The geometries of reactants, products, intermediates, and TSs were fully optimized without symmetry constraints by the energy gradient methods. All optimized geometries were obtained by using the HF, MP2,[15] and the Becke 3LYP(B3LYP) hybrid density functional[16,17] with the 6-31++G(2d,p) (split-valence plus diffuse functions plus 2dp-polarization functions[18,19]) basis set. Vibrational frequencies were calculated by using the analytical second derivatives at the HF/6-31++G(2d,p), the MP2/6-31++G(2d,p), and the B3LYP/6-31++G(2d,p) levels to confirm the stationary structures and to correct for the zero-point vibrational energy. The values of harmonic vibrational frequencies determined at various levels have been scaled by 0.8929 at HF/6-31++G(2d,p), 0.9434 at MP2/6-31++G(2d,p), and 0.9613 at B3LYP/6-31++G(2d,p).[20] Intrinsic reaction coordinate (IRC) calculations using internal coordinates[21−23] were performed to verify that computed transition states were saddle points between reactants and products. Atomic charge distributions were calculated by the atoms in molecule (AIM) theory by Bader[24] using AIM2000.[25]

3. Results and Discussion

3.1. Geometrical Difference between the Crystal Structure and the Optimized Structure of UN. First of all, we carried out a full geometry optimization for the isolated UN molecule in comparison with the crystal structure of UN. Figure 1 shows molecular structure of UN in the crystalline state.[26] UN can be crystallized in only one form, to the best of our knowledge. The crystal structure of UN has been determined by neutron

diffraction.[26] The crystal structure of UN shows that the acidic proton is attached to the carbonyl oxygen atom of urea and forms a strong hydrogen bond to an oxygen atom of the nitrate ion. The C−O distance, 1.298(2) Å, and the C−N distances, 1.312-(1) Å, are longer and shorter, respectively, than the corresponding distances in urea.[26] The acidic proton is on the carbonyl oxygen atom with an O−H distance of 1.006(3) Å. However, the acidic proton in the optimized geometry of UN at the HF/6-31++G(2d,p), the MP2/6-31++G(2d,p), and the B3LYP/6-31++G(2d,p) levels is not located on the carbonyl oxygen atom, as shown in Figure 2. The optimized geometry of UN is stable compared to the sum of the optimized urea and nitric acid molecules by 13.4 kcal/mol at the HF/6-31++G(2d,p) level and by 14.0 kcal/mol at the MP2/6-31++G(2d,p) level. The optimized C−O distance, 1.238 Å, and the C−N distances, 1.364 Å (at the MP2/6-31++G(2d,p) level), are shorter and longer, respectively, than the corresponding distances in crystalline UN. Thus, it is found that there is a considerable geometrical difference between the crystal structure and the optimized geometry of UN.

To investigate the effect of the acidic proton located on the carbonyl oxygen atom, we performed calculations for optimized geometries of urea and $(NH_2)_2COH^+$ (the acidic proton is attached to the carbonyl oxygen atom of urea) at the MP2/6-31++G(2d,p) level. The results are shown in Figure 3a,b. When $(NH_2)_2COH^+$ is formed by the attachment of the proton on the carbonyl group in urea, the C−O bond is longer, 1.312 Å, relative to that of urea, 1.221 Å, and the C−N bond is shorter, 1.326 and 1.320 Å, respectively, relative to that of urea, 1.389 Å. Therefore, judging from the optimized geometries described above, the crystal structure of UN is similar to that of $(NH_2)_2COH^+$. Furthermore, we attempted to analyze the atomic charge distributions and the covalent bond orders by using the theory of AIM at the MP2/6-31++G(2d,p) level. Parts a−c of Figure 4 show the atomic charge distributions and the atomic overlap matrix (AOM)-derived covalent bond orders of UN, urea, and $(NH_2)_2COH^+$, respectively. Table 1 lists C−O and C−N distances and the covalent bond orders in the optimized geometry of urea, UN, and $(NH_2)_2COH^+$ at the MP2/6-31++G-(2d,p) level and the experimental values.[26] In Figure 4c, the atomic charge of the carbonyl oxygen atom of $(NH_2)_2COH^+$ is higher (−1.1434) than that of urea (−1.2162). The covalent bond order of C−O bond in $(NH_2)_2COH^+$ is lower (0.8830) than that of urea (1.2115), whereas the covalent bond order of C−N bond in $(NH_2)_2COH^+$ is higher (1.1559, 1.1621) than that of urea (1.0096). Therefore, the double bond character of the C−O bond in $(NH_2)_2COH^+$ decreases with an increase in the double bond character of the C−N bond in comparison with those of urea. These results can be linked with the results of the C−O and C−N distances in the optimized geometries of UN and $(NH_2)_2COH^+$, as shown in Table 1. That is, when the acidic proton is attached to the carbonyl oxygen atom of urea, each C−N bond in $(NH_2)_2COH^+$ acquires, through resonance, more double bond character.

It should be pointed out that the double bond character of these C−N bonds in the crystal structure of UN is considerably increased in comparison to that in the optimized geometry of UN. Furthermore, the values of the total energy of the optimized geometries of UN($(NH_2)_2CO + HNO_3$) and $(NH_2)_2COH^+ + NO_3^-$ predict that former is more stable by 130.8 kcal/mol at the MP2/6-31++G(2d,p) level.

However, in the crystal structure of UN by neutron diffraction,[26] this hydrogen bond of the O−H- - -O type and four other hydrogen bonds of the N−H- - -O type, join the uronium and nitrate ions into the two-dimensional network. Therefore, we presumed that the high stability of the UN crystal can be explained by the two-dimensional hydrogen bonds network.

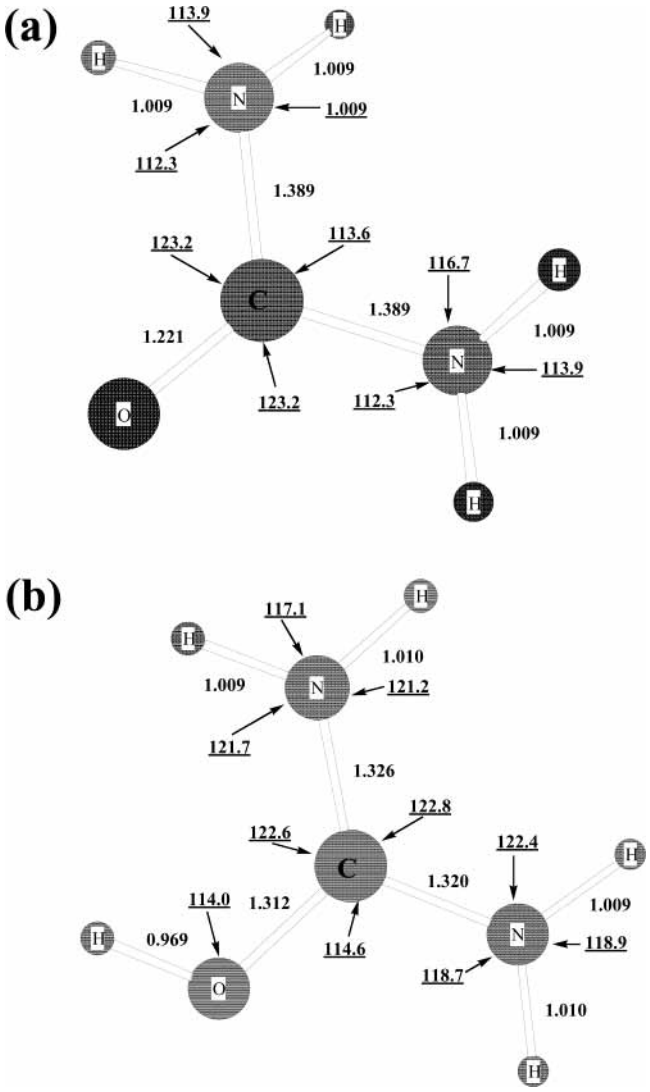

Figure 3. MP2/6-31++G(2d,p) optimized geometries of urea (a) and $(NH_2)_2COH^+$ (b). Bond distances are in ångstroms, and angles (underlined) are in degrees.

TABLE 1: Optimized C−O and C−N Bond Lengths of Urea Nitrate and Some Related Compounds (MP2/6-31++G(2d,p) Level)

	C−O bond length (Å)		C−N(1) bond length (Å)		C−N(2) bond length (Å)	
compound	opt	obs[a]	opt	obs[a]	opt	obs[a]
urea nitrate	1.238 (1.1192)[b]	1.298	1.364 (1.0651)	1.312	1.374 (1.0330)	1.315
urea	1.221 (1.2115)	1.243	1.389 (1.0096)	1.351	1.389 (1.0096)	1.351
$(NH_2)_2COH^+$	1.312 (0.8830)		1.326 (1.1559)		1.320 (1.1621)	

[a] The observed values are in the bond length in crystal.[26] [b] Number in parentheses stand for AOM-derived covalent bond order.

3.2. Vibrational Spectra of UN. The experimental infrared spectrum of UN is shown in Figure 5a. The ab initio calculated and experimental vibrational frequencies for UN are compared in Table 2. The calculated IR spectrum at the MP2/6-31++G-(2d,p) level is presented in Figure 5b, whereas the corresponding

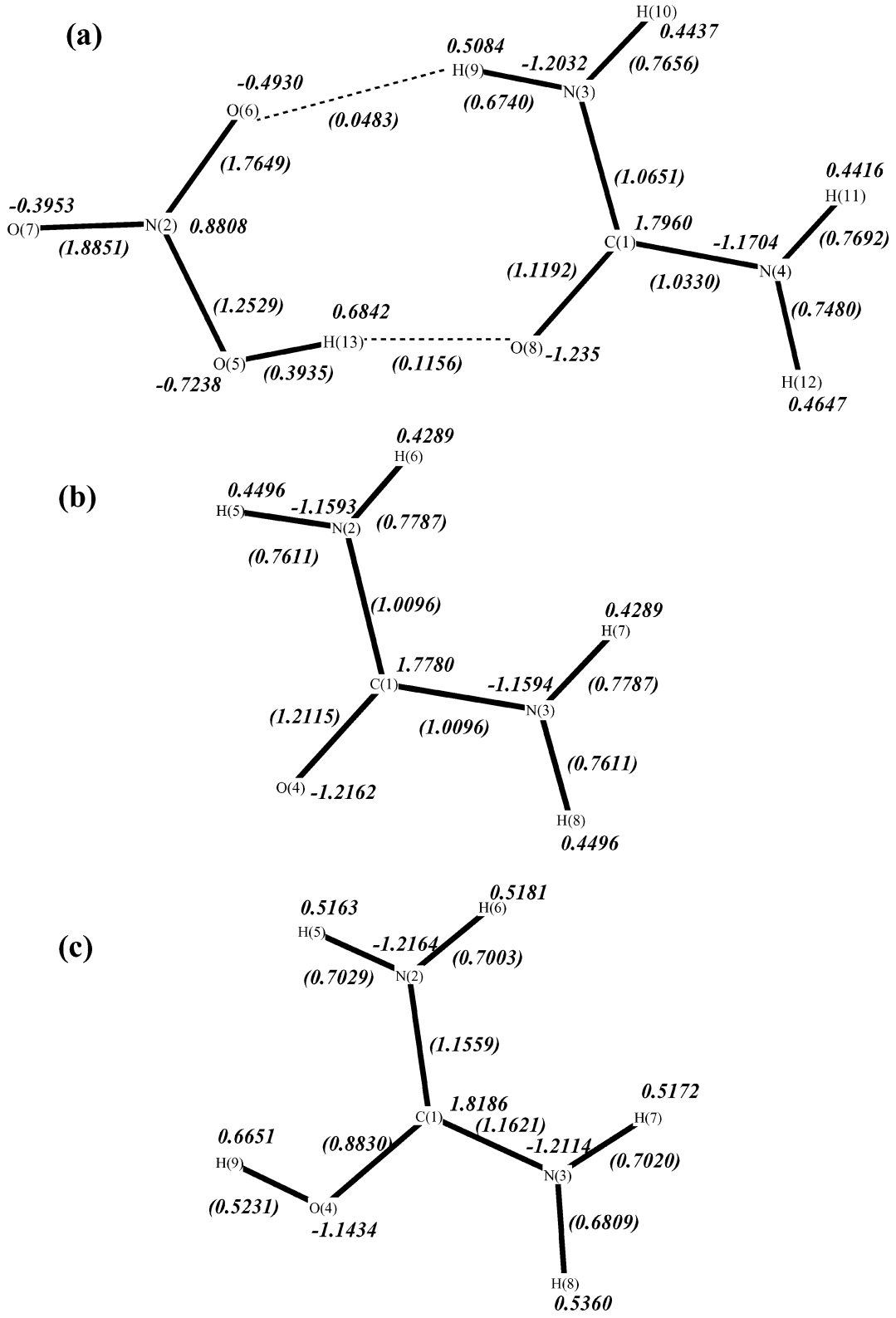

Figure 4. Atomic charge distributions of UN, urea, and $(NH_2)_2COH^+$ calculated at the MP2/6-31++G(2d,p) level. Numbers in parentheses stand for AOM-derived covalent bond orders.

eigenvectors are given in Figure 6. The observed band frequencies and integrated intensities were compared with the theoretical calculations to make the assignments. There are strong bands around 3414−3365 and 3257−3205 cm^{-1}. The former bands are assigned to asymmetric stretching of NH_2, and the latter bands are assigned to symmetric stretching of NH_2.

The spectrum of UN exhibits broad bands due to the symmetric stretching of C═O- - -H- - -ONO_2 around 3000- - 2000 cm^{-1} compared to 2869. 9 cm^{-1} calculated at the MP2 level. This broad feature leads us to speculate that the UN crystal has the structure of strong intermolecular interactions in connection with the acidic proton on the carbonyl oxygen atom. There is agreement between the calculated and experimental values for mode 27, which involves the C═O symmetric stretching motion; the observed value is 1678 cm^{-1} compared to 1655.1 cm^{-1} calculated at the MP2 level.

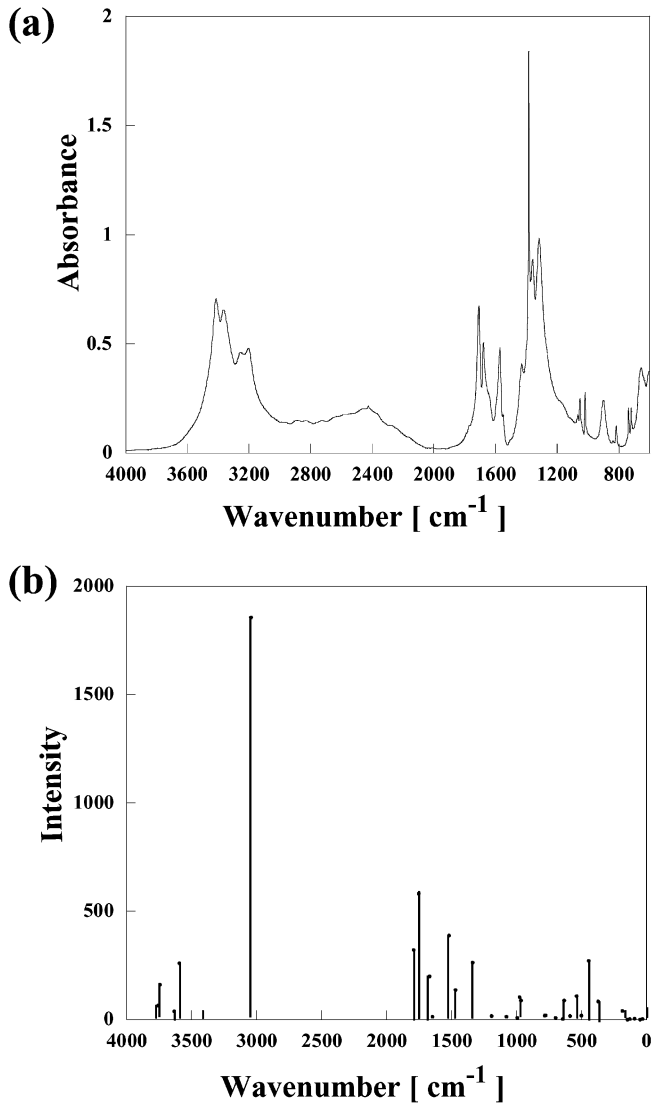

Figure 5. (a) Infrared spectrum of the urea nitrate at room temperature. (b) Theoretical IR spectra of the urea nitrate molecule calculated at the MP2/6-31++(2d,p) level.

3.3. Reaction Pathway of UN. We carried out ab initio MO calculations including the electron correlation to determine the reaction pathways. Two transition states and an intermediate were determined. Parts a−c of Figure 7 show geometries of transition states and an intermediate product for the decomposition reaction paths of UN optimized at the MP2/6-31++G(2d,p) level. Figure 7a shows the optimized geometry of a transition state (TS(1)) for beginning an internal proton-transfer reaction, the arrows indicate the displacement vectors of the normal mode with imaginary frequency. TS(1) is a four-member ring. The potential energy profile for the UN decomposition mechanism is illustrated in Figure 8. The vibrational frequency (1762.7i cm^{-1}) corresponds to the H- - -N(3) stretching mode leading to an internal proton-transfer reaction. After TS(1), an intermediate (INT(1), Figure 7b) is formed by internal proton transfer. By IRC (intrinsic reaction coordinate) calculations, the direction from TS(1) to INT(1) have been confirmed. These IRC calculations show that the transition state TS(1) is a saddle point connecting the reactant and the product (INT(1)). This process, UN → TS(1) has a potential energy barrier of 47.8 kcal/mol. Furthermore, a transition state TS(1) was obtained only from the optimized structure of UN. We searched for the TS(1) for an internal proton-transfer reaction from $(NH_2)_2COH^+$ (where the acidic proton is attached to the carbonyl oxygen atom of urea, a moiety in the crystal structure of UN), but these calculations did not lead to an internal proton-transfer reaction. $(NH_2)_2COH^+$ did not proceed to TS(1). These results can be linked with the results mentioned in the previous paragraph. When the acidic proton is attached to the carbonyl oxygen atom of urea, the double bond character of these C−N bonds in the crystal structure of UN considerably increased in comparison with the optimized geometry of UN. Therefore, in this instance, a $(NH_2)_2COH^+$ formation of a four-member N- -H- -N−C ring does not seem to occur in an internal proton-transfer reaction by strong double bond character of these C−N bonds. In the optimized geometry of UN a more effective four-member interaction will occur, as shown in Figure 7a. Subsequently, INT(1) proceeds to TS(2) (319.3i cm^{-1}, Figure 7c). The directions of the displacement vectors of TS(2) strongly indicate the occurrence of the decomposition to produce NH_3, HNCO, and HNO_3. The potential energy for this reaction is 1.5 kcal/mol. Therefore, after TS(2) is produced, NH_3, HNCO, and HNO_3 should be rapidly generated. These results strongly suggest that this decomposition occurs via internal hydrogen transfer from one of the amino groups to the other, i.e., proton transfer from NH_2 to produce NH_3. Subsequently, HNCO forms accompanied by $NH_3 + HNO_3$ or AN. In our present calculations, the route to reaction channel (1) is clearly defined quantum chemically.

The UN crystal is a considerably stable energetic material that releases energy in an explosive reaction. The present study finds that in an early stage of UN decomposition, transition state

TABLE 2: Calculated and Experimental Vibrational Frequencies of Urea Nitrate

mode	HF/6-31++ G(2d,p)[a]	B3LYP/6-31++ G(2d,p)[b]	MP2/6-31++ G(2d,p)[c]	exp
1	40.6	36.6	29.8	no
2	46.5	51.9	47	no
3	86.8	93.2	87.2	no
4	98.3	123.2	120.2	no
5	138.1	152.7	139.1	no
6	160.5	193.6	176.5	no
7	337.4	328.1	351.1	no
8	400.9	395.6	420.2	no
9	476.6	471.8	470.9	no
10	487.2	486.4	508.9	534
11	559.8	574.2	554.7	550
12	586.3	623.1	598.5	573
13	652.6	628	608.1	637
14	714.9	677.2	659.4	656
15	773.2	743.2	732.6	719
16	828.6	764.2	739.7	737
17	848.6	949.3	911	815
18	948.5	951.3	923.9	899
19	1033.9	963.3	939.4	1018
20	1045.7	1022.7	1016.5	1052
21	1146.9	1131.3	1124.1	1165
22	1396	1279.1	1263.1	1317
23	1405.3	1410.1	1388.2	1385
24	1439.9	1439.7	1434.2	1430
25	1588.7	1564.6	1555.7	1571
26	1603.7	1582.7	1574.4	1591
27	1686.7	1653.4	1655.1	1678
28	1712.6	1661.8	1689.6	1709
29	3130.5	2671.9	2869.9	broad
30	3400.5	3390.7	3391.7	3205
31	3415.7	3454.7	3426.9	3257
32	3520.2	3547.5	3532.6	3365
33	3525.5	3570.2	3547.7	3414

[a] Values scaled by 0.8929. [b] Values scaled by 0.9613. [c] Values scaled by 0.9434.

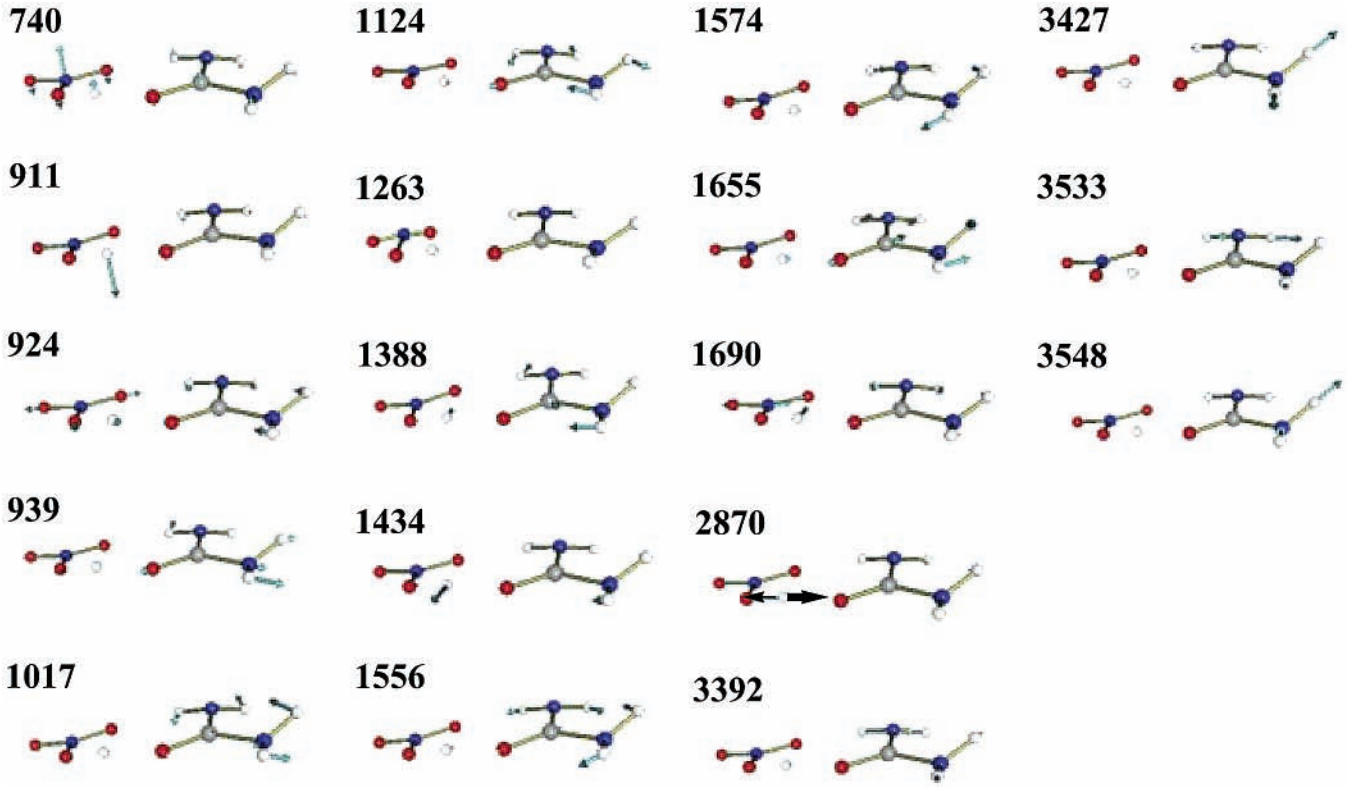

Figure 6. Normal mode eigenvectors for the urea nitrate molecule obtained at MP2/6-31G++(2d,p)level. The indicated numbers correspond to the scaled values of the frequencies (3548 to 740 cm^{-1}).

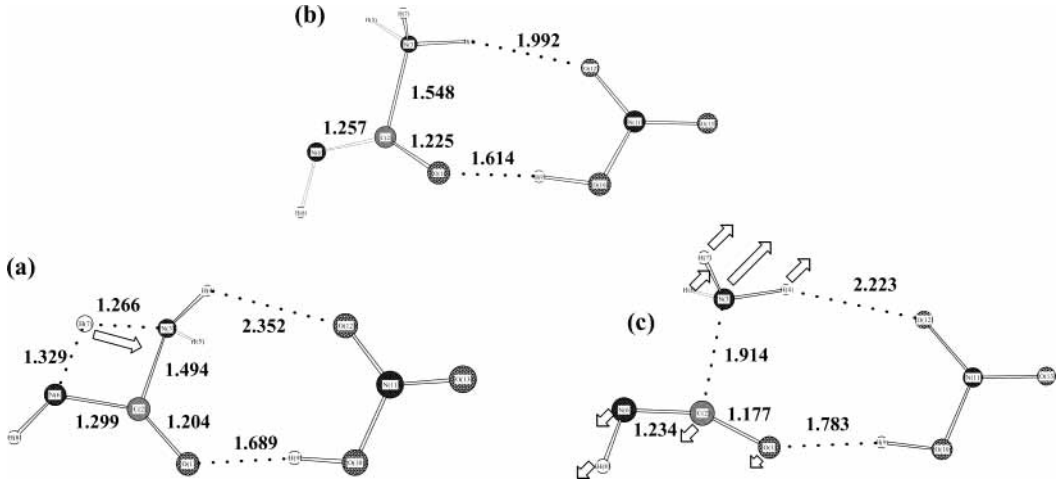

Figure 7. (a) MP2/6-31++G(2d,p) optimized geometries and displacement vectors of the normal mode with an imaginary frequency (1762.7i cm^{-1}) for the transition state (TS1). Bond distances are in ångstroms. (b) MP2/6-31++G(2d,p) optimized geometry of intermediate (1). Bond distances are in ångstroms, and angles (underlined) are in degrees. (c) MP2/6-31++G(2d,p) optimized geometries and displacement vectors of the normal mode with an imaginary frequency (319.2i cm^{-1}) for the transition state (TS2). Bond distances are in ångstroms.

TS(1) is reached only from the optimized structure of UN. However, $(NH_2)_2COH^+$ (a moiety in the crystal structure of UN) does not proceed to TS(1) by an internal proton-transfer reaction. This leads us to speculate that the two-dimensional strong hydrogen-bond network of the UN crystal always needs to be destroyed by significant structural relaxation due to external stimuli (e.g., heat or impact) before the beginning of the decomposition reactions of UN. Hydrogen-bond networks may play an important role in "stabilizing" energetic materials.

4. Conclusions

In our present calculations, it is found that there is a considerable geometrical difference between the crystal structure and the optimized structure of gas-phase UN. At TS(1), a four-member ring was obtained only from the optimized structure of UN. In the crystal structure of UN, formation of a four-member ring does not seem likely to occur by internal proton transfer due to the reaction by the strong double-bond character of these C−N bonds. Thus, we speculate that the hydrogen-bond network in the UN crystal plays an important role in its considerable stability. There are three important products (NH_3, HNCO, and HNO_3) of the thermal decomposition reaction of UN. This study has revealed a series of UN reaction paths through one intermediate and two transition states with the evolution of the initial gaseous species, NH_3, HNCO, and HNO_3, in that order. It was shown that there is a reaction pathway for

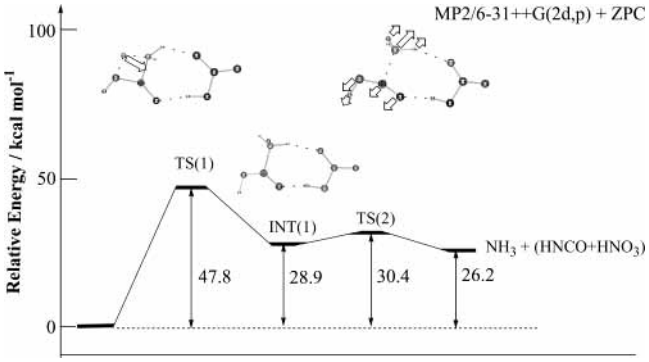

Figure 8. Potential energy profile of UN decomposition.

the production of NH_3 through the decomposition reaction with a potential energy barrier of about 47.8 kcal/mol at the MP2/6-31++G(2d,p) level. These calculated results seem to support the experimental results[13] that were observed at the thermal decomposition of UN by using *T*-jump/FT-IR spectroscopy.

Acknowledgment. We thank the Institute for Nonlinear Science and Applied Mathematics at Hiroshima University for the use of a COMPAQ Personal Workstation 433au, and Okazaki National Research Institutes for the use of the Fujitsu VPP5000. We also thank Prof. T. B. Brill of University of Delaware; Dr. H. Arisawa of Technical Department, Technical Research and Development Institute, Japan Defense Agency; and General Manager I. Omura and Dr. N. Nagayasu of Chugoku Kayaku Co., Ltd. for helpful discussions. We thank the reviewers for some comments and kind correction of the syntax of manuscript toward traditional western usage. This study is supported by a Grant-in-Aid on research for the future "Photoscience" (JSPS-RFTF-98P01202) from the Japan Society for the Promotion of Science.

References and Notes

(1) Politzer, P.; Alper, H. E. *Computational Chemistry, Reviews of current trends;* Leszczynski J., Ed.; World Scientific: Singapore, 1999; Vol. 4, Chapter 6.

(2) Hiyoshi, R. I.; Nakamura, J. *Proc. Int. Symp. Anal. Det. Expl., 6th* **1998**, p 15.

(3) Hiyoshi, R. I.; Nakamura, J. *Kayaku Gakkaishi* **2000**, *61* (3), 120.

(4) Kontoyianni, M.; Bowen, P. *J. Comput. Chem.* **1992**, *13*, 657.

(5) Meier, R. J.; Coussens, B. *THEOCHEM* **1992**, *85*, 25.

(6) Gobbi, A.; Frenking, G. *J. Am. Chem. Soc.* **1993**, *115*, 2362.

(7) Dixon, D. A.; Matsuzaga, N. *J. Phys. Chem.* **1994**, *98*, 3967.

(8) Ramondo, F.; Bencivenni, L.; Rossi, V.; Caminiti, R. *THEOCHEM* **1992**, *277*, 185.

(9) Godfrey, P. D.; Brown, R. R.; Hunter, A. N. *J. Mol. Struct.* **1997**, *413*, 405.

(10) Masunov, A.; Dannenberg, J. J. *J. Phys. Chem.* **1999**, *A 103*, 178.

(11) Masunov, A.; Dannenberg, J. J. *J. Phys. Chem.* **2000**, *B 104*, 806.

(12) Kohno, Y.; Takahashi, O.; Saito, K. *Phys. Chem. Chem. Phys.* **2001**, *3*(14) 2742.

(13) Hiyoshi, R. I.; Brill, T. B.; Kohno, Y.; Takahashi, O.; Saito, K. *Int. Detonation Symp, 12th* **2002**, in press.

(14) Frisch, M. J.; Trucks, G. W.; Schlegel, H. B.; Scuseria, G. E.; Robb, M. A.; Cheeseman, J. R.; Zakrzewski, V. G.; Montgomery, J. A., Jr.; Stratmann, R. E.; Burant, J. C.; Dapprich, S.; Millam, J. M.; Daniels, A. D.; Kudin, K. N.; Strain, M. C.; Farkas, O.; Tomasi, J.; Barone, V.; Cossi, M.; Cammi, R.; Mennucci, B.; Pomelli, C.; Adamo, C.; Clifford, S.; Ochterski, J.; Petersson, G. A.; Ayala, P. Y.; Cui, Q.; Morokuma, K.; Malick, D. K.; Rabuck, A. D.; Raghavachari, K.; Foresman, J. B.; Cioslowski, J.; Ortiz, J. V.; Stefanov, B. B.; Liu, G.; Liashenko, A.; Piskorz, P.; Komaromi, I.; Gomperts, R.; Martin, R. L.; Fox, D. J.; Keith, T.; Al-Laham, M. A.; Peng, C. Y.; Nanayakkara, A.; Gonzalez, C.; Challacombe, M.; Gill, P. M. W.; Johnson, B. G.; Chen, W.; Wong, M. W.; Andres, J. L.; Head-Gordon, M.; Replogle, E. S.; Pople, J. A. *Gaussian 98*, revision A.11.1; Gaussian, Inc.: Pittsburgh, PA, 1998.

(15) Mϕller, C.; Plesset, M. S. *Phys. Rev.* **1934**, *46*, 618.

(16) Becke, A. D. *J. Chem. Phys.* **1993**, *98*, 5648.

(17) Lee, C.; Yang, W.; Parr, R. G. *Phys. Rev.* **1988**, *B41*, 785.

(18) (a) Hehre, W. J.; Ditchfield, R.; Pople, J. A. *J. Chem. Phys.* **1972**, *56*, 2257. (b) Frankl, M. M.; Pietro, W. J.; Hehre, W. J.; Binkley, J. S.; Gordon, M. S.; DeFees, D. J.; Pople, J. A. *J. Chem. Phys.* **1982**, *77*, 3654.

(19) Hariharan, P. C.; Pople, J. A. *Theor. Chem. Acta* **1973**, *28*, 213.

(20) Forseman, J. B.; Frisch, A. In *Exploring Chemistry with Electronic Structure Methods*; Gaussian, Inc.: Pittsburgh, PA, 1996.

(21) Gonalez, C.; McDouall, J. J. W.; Sclegel, H. B. *J. Phys. Chem.* **1990**, *94*, 7467.

(22) Gonalez, C.; Sclegel, H. B. *J. Chem. Phys.* **1989**, *90*, 2154.

(23) Fukui, K. *Acc. Chem. Res.* **1981**, *14*, 363.

(24) Bader, R. F. W. *Atoms in Molecules: A Quantum Theory*; Clarendon Press: Oxford, U.K., 1990.

(25) Biegler-König; Bayles, D. *J. Comput. Chem.* **2001**, *22*, 545.

(26) Worsham, J. E.; Busing, W. R. *Acta Crystallogr.* **1969**, *B25*, 572.